CONFERENCE PRE-PRINT

EXPERIMENTAL STUDY ON THE MIGRATION PROCESS OF ADATOM IN THE GROWTH DYNAMIC OF FUZZ

Z. LIU, Z.S. GAO, Y.Y. LI, L. LI, Z. CHEN, C. YIN, S.F. MAO, M.Y. YE* University of Science and Technology of China Hefei, China Email: yemy@ustc.edu.cn

Abstract

Tungsten (W) is considered the most promising candidate for plasma-facing materials (PFM) in fusion devices. The fusion community has observed a concerning phenomenon on the W surface induced by helium (He) ions, known as "fuzz", over the past two decades. This surface modification degrades the property of W, influencing the life of PFMs. In this study, we design a special sample structure with deposited W film on silicon (Si) substrates to reveal adatom migration during surface evolution. The samples are irradiated by He plasma in CLIPS with the conditions as: E_i is 75 eV, T_s is 850 K, and He ion fluence, Φ_{He} , is 5 × 10²⁵ m⁻². The results show that the surface and substrate materials intermingle during fuzz formation.

1. INTRODUCTION

Tungsten (W) is considered the most promising candidate material for divertors in fusion devices due to its exceptional physical and chemical properties, including a high melting point, low sputtering coefficient, and good thermal conductivity. Over the past two decades, the fusion community has observed a concerning phenomenon on the W surface, known as "fuzz" [1], induced by helium (He), a by-product of nuclear fusion reactions between deuterium and tritium.

It is widely accepted that fuzz formation is linked to the presence of He bubbles, which result from a combination of processes in the initial stages, such as He atom penetration into the material, atomic diffusion, trapping at thermal vacancies, and subsequent bubble formation and aggregation [2]. However, there is ongoing debate regarding whether He and W migration are the rate-limiting step during late-stage fuzz growth and the specific mechanisms by which He and W migration occurs [3-6].

In this study, we experimentally investigate the adatom migration process during fuzz growth. Surface morphologies and features were observed and analyzed. The results show that the surface and substrate materials intermingle during fuzz formation, suggesting that He bombardment contribute to the creation of adatoms, which transport material from the bulk to the surface.

2. EXPERIMENTAL

The irradiation experiments are conducted in the linear plasma device, CLIPS, of which the detailed description can be found in our previous work [7-9]. The steady-state He plasma is generated by a Philips ionization gauge (PIG) discharge using a LaB₆ cathode that is heated by a direct current. The base pressure in the vacuum chamber is 5×10^{-5} Pa and the working pressure during plasma irradiation is maintained at 1.5 Pa. Fig. 1 depicts the schematic diagram of the experimental setup. The samples are placed downstream perpendicular to the magnetic field line. The magnetic field strength is approximately 0.01 T, which suppresses the radial diffusion of the plasma and results in a high-density plasma. The typical electron density n_e is on the order of 10^{18} m⁻³, and the electron temperature of the center of the plasma column is $T_e \sim 8.5$ eV. The He ion flux to the samples is measured using an electrostatic probe located around 10 mm upstream from the sample, and the He flux is fixed at 1.7×10^{22} m⁻² s⁻¹ in this experiment. The samples are electrically biased in the He plasma with a potential of +5.0 V, and the incident ion energy, E_i , which is determined by the potential difference between the sample and the plasma space potential, is controlled by changing the biasing voltage. The He ion incident direction is approximately normal to the sample surface due to acceleration in the sheath. The Si samples are mounted on a water-cooling stage, and the surface temperature, T_s , is measured using a K-type thermocouple. To ensure a good thermal connection, the head of the thermocouple presses against the back of the sample.

In this study, commercial P-type (100) Si samples ($10 \times 10 \times 1 \text{ mm}^3$) with an electrical resistivity of $\sim 0.001 \ \Omega \cdot \text{cm}$ are used as substrates. A magnetron sputtering apparatus was utilized to deposit 1 to 10 nm thick tungsten thin films onto the substrates. Before processing, the Si samples are cleaned with acetone, ethanol, and deionized water, successively. The deposition process is controlled by adjusting the deposition rate (0.014 nm/s in this case) of the magnetron sputtering device and deposition time, which leads to a sub-monolayer with an average thickness of approximately 0.4 nm. The He plasma irradiation conditions are as follows: E_i is 75 eV, T_s is 850 K, and He ion fluence, ϕ_{He} , is $5 \times 10^{25} \ \text{m}^{-2}$. After the plasma irradiation, the surface morphology analysis is carried out via a Hitachi SU8220 Field Emission Scanning Electron Microscope (FE-SEM).

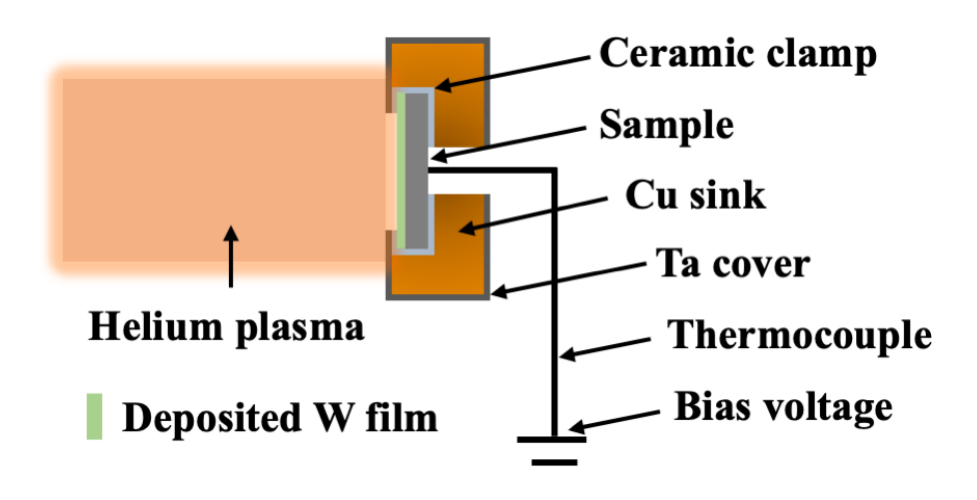


FIG. 1. Schematic view of the experimental setup in the He plasma irradiation experiment.

3. RESULTS AND DISCUSSION

FIG. 2(a)-(c) illustrates the top-view FE-SEM images of the sample surface irradiated by He plasma under conditions of $E_i = 75$ eV, $T_s = 850$ K, $\Phi_{He} = 5 \times 10^{25}$ m⁻², with different W film thicknesses ranging from 1 nm to 10 nm. FIG. 2(d)-(f) present the corresponding 45-degree tiled images. The sample surface in the presence of a 1 nm W film presents the formation of cone arrays under He plasma irradiation. The irradiated surface is covered by densely distributed cones, exhibiting smooth sides and sharp tips. The cones extend perpendicular to the surface, oriented in the direction of incident He ions, which are accelerated by the electric field within the sheath. When the thickness of tungsten increases to 5 nm and 10 nm, the color of the sample surface becomes darker under the naked eye. The SEM image shows that the nanostructure on the surface of the sample changes from nanocones to nanopillars.

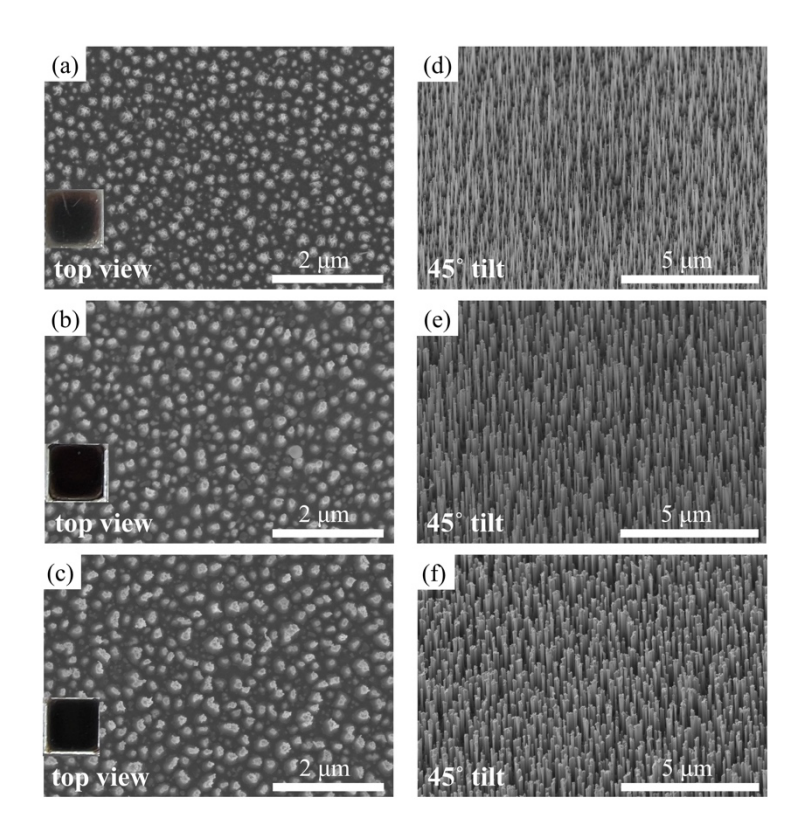


FIG. 2. The top view and 45-degree tiled FE-SEM images of sample surfaces irradiated by He plasma with 1 nm((a) and (d)), 5 nm((b) and (e)), and 10 nm((c) and (f)) pre-deposited W film. The samples are irradiated under conditions of $E_i = 75$ eV, $T_s = 850$ K, and $\Phi_{He} = 5 \times 10^{25}$ m².

The magnified images under the electron microscope reveal the complex shapes of these nanopillars. FIG. 3(a)-(c) illustrates the tiled view of FE-SEM images of the sample surface irradiated by He plasma under conditions of $E_i = 75$ eV, $T_s = 850$ K, $\Phi_{He} = 5 \times 10^{25}$ m⁻², with W film thicknesses of 5 nm and 10 nm. At the top of the densely arranged nanopillars, there are bent and intertwined nanofibers growing, which are very similar to the fuzz structure that grows on the pure tungsten surface. For the formation of the fuzz structure at the top of the nanostick, the temperature parameter is less than the typical parameter range for its formation, which is between 1000 K and 2000 K. This result indicates that there is a significant temperature difference between the top of the nanocolumn and the surface of the sample.

FIG. 4 presents the EDX analysis results of the fuzz structure at the top of the nanocolumn. The EDX results indicate that these fuzzy structures are composed of W and Si. An intriguing phenomenon was observed for samples with 100 nm tungsten coatings on Si substrates. Compared to pure tungsten, the fuzz growth rate is faster under the same irradiation dose. This suggests that the substrate atoms play a role as adsorbents in the complex migration process involved in fuzz growth.

From the consistent morphology of the nanotubes and the formation of the nanowire structure at the top of the tubes, it can be seen that the bombardment position of the incident helium ions should be distributed throughout the entire nanoscale structure. The migration process may involve both diffusion processes and direct ballistic penetration processes. At the same time, the mechanism of the formation of adsorbed atoms may not only include the process of helium bubble rupture, but also other physically factor-driven diffusion processes towards the top of the nanoscale structure.

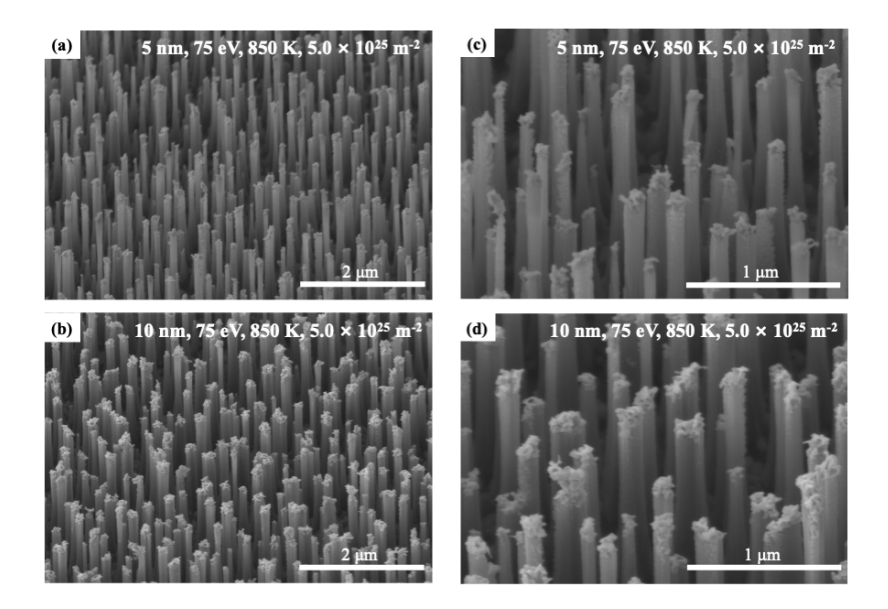


FIG. 3. The 45-degree tiled FE-SEM images of sample surfaces irradiated by He plasma with 5 nm((a) and (c)) and 10 nm((b) and (d)) pre-deposited W film. The samples are irradiated under conditions of $E_i = 75$ eV, $T_s = 850$ K, and $\Phi_{He} = 5 \times 10^{25}$ m⁻².

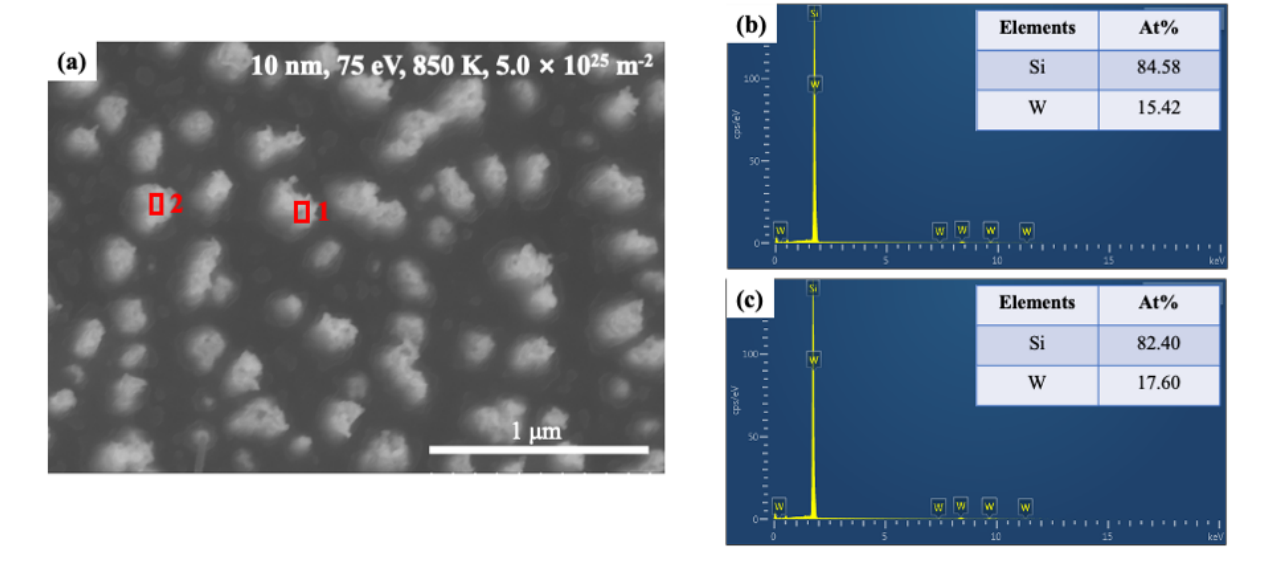


FIG. 4. (a) The SEM images of sample surfaces irradiated by He plasma with 10 nm pre-deposited W film. The samples are irradiated under conditions of $E_i = 75$ eV, $T_s = 850$ K, and $\Phi_{He} = 5 \times 10^{25}$ m⁻². (b) The EDX

4. CONCLUSIONS

In this study, we experimentally investigate the adatom migration process during fuzz growth. Surface morphologies and features were observed and analyzed. The results show that the surface and substrate materials intermingle during fuzz formation, suggesting that He bombardment contribute to the creation of adatoms, which transport material from the bulk to the surface.

ACKNOWLEDGEMENTS

This work was supported by the Joint Funds of the National Natural Science Foundation of China (NSFC) (Grant No. U2267208). We acknowledge the USTC Center for Micro and Nanoscale Research and Fabrication for supporting the surface morphology analysis.

REFERENCES

- [1] Bolt, H., Barabash, V., Krauss, W., Linke, J., Neu, R., Suzuki, S., Yoshida, N. and ASDEX Upgrade Team, 2004. Materials for the plasma-facing components of fusion reactors. Journal of nuclear materials, 329, pp.66-73.
- [2] Kajita, S., Ito, A.M. and Ibano, K., 2022. Growth of fiberform nanostructures on metal surfaces by helium plasma irradiation. Journal of Applied Physics, 132(18).
- [3] Doerner, R.P., Nishijima, D., Krasheninnikov, S.I., Schwarz-Selinger, T. and Zach, M., 2018. Motion of W and He atoms during formation of W fuzz. Nuclear Fusion, 58(6), p.066005.
- [4] Trufanov, D., Marenkov, E. and Krasheninnikov, S., 2015. The role of the adatom diffusion in the tungsten fuzz growth. Physics Procedia, 71, pp.20-24.
- [5] Patino, M.I., Nishijima, D., Tokitani, M., Nagata, D. and Doerner, R.P., 2020. Material mixing during fuzz formation in W and Mo. Physica Scripta, 2020(T171), p.014070.
- [6] Wright, J.A., 2022. A review of late-stage tungsten fuzz growth. Tungsten, 4(3), pp.184-193.
- [7] Liu, Z., Li, L., Gao, Z., Chen, Z., Yin, C., Mao, S., Kajita, S., Ohno, N. and Ye, M., 2024. Cone array formation on Si surfaces by low-energy He plasma irradiation with magnetron sputtering pre-deposited Ta. Journal of Applied Physics, 135(9).
- [8] Liu, Z., Li, L., Gao, Z., Chen, Z., Yin, C., Mao, S., Kajita, S., Ohno, N. and Ye, M., 2024. Nanopatterning of Si surfaces by normal incident He plasma irradiation. Applied Physics Letters, 124(10).
- [9] Li, L., Liu, Z., Chen, Z., Yin, C., Mao, S., Wu, X., Ohno, N. and Ye, M., 2024. Surface modification of ZrC dispersion-strengthened W under low energy He plasma irradiation. Nuclear Fusion, 64(5), p.056008.